

# Narrowband NIR-Induced *In Situ* Generation of the High-Energy *Trans* Conformer of Trichloroacetic Acid Isolated in Solid Nitrogen and its Spontaneous Decay by Tunneling to the Low-Energy *Cis* Conformer

R. F. G. Apóstolo,<sup>1</sup> R. R. F. Bento,<sup>1,2</sup> R. Fausto<sup>1,\*</sup>

<sup>1</sup> Department of Chemistry, University of Coimbra, P 3004–535, Coimbra, Portugal

<sup>2</sup> Instituto de Física, Universidade Federal de Mato Grosso, 78060-900, Cuiabá, Brazil

\* Corresponding author's e-mail address: rfausto@ci.uc.pt

RECEIVED: July 20, 2015 \* REVISED: October 8, 2015 \* ACCEPTED: October 10, 2015

THIS PAPER IS DEDICATED TO DR. SVETOZAR MUSIĆ ON THE OCCASION OF HIS 70<sup>TH</sup> BIRTHDAY

**Abstract:** The monomeric form of trichloroacetic acid (CCl<sub>3</sub>COOH; TCA) was isolated in a cryogenic nitrogen matrix (15 K) and the higher energy *trans* conformer (O=C–O–H dihedral: 180°) was generated *in situ* by narrowband near-infrared selective excitation the 1<sup>st</sup> OH stretching overtone of the low-energy *cis* conformer (O=C–O–H dihedral: 0°). The spontaneous decay, by tunneling, of the generated high-energy conformer into the *cis* form was then evaluated and compared with those observed previously for the *trans* conformers of acetic and formic acids in identical experimental conditions. The much faster decay of the high-energy conformer of TCA compared to both formic and acetic acids (by ~35 and *ca.* 25 times, respectively) was found to correlate well with the lower energy barrier for the *trans* → *cis* isomerization in the studied compound. The experimental studies received support from quantum chemistry calculations undertaken at the DFT(B3LYP)/cc-pVDZ level of approximation, which allowed a detailed characterization of the potential energy surface of the molecule and the detailed assignment of the infrared spectra of the two conformers.

**Keywords:** trichloroacetic acid, NIR-induced *in situ* generation of the higher energy *trans*-TCA conformer, spontaneous decay by tunneling, matrix-isolation infrared spectroscopy, quantum chemical calculations.

## 1. INTRODUCTION

THE first report on an infrared-induced conformational isomerization in a cryomatrix was presented by Hall and Pimentel in 1963.<sup>[1]</sup> That work considered the isomerization of HONO upon broadband infrared excitation. However, the generalization of the technique was initially severely conditioned by the usual similarity between the vibrational spectra of different conformers. It was only *ca.* 40 years later that the technique evolved to an extremely effective and elegant strategy for optically controlling the populations of different conformers of a molecule. For that, the use of narrowband tuneable lasers as excitation source

was introduced.<sup>[2–4]</sup> It is now possible to choose the vibrational mode used to excite the targeted precursor conformer in a very selective way,<sup>[2–8]</sup> and since then many successful examples of application of the technique have been reported.<sup>[2–12]</sup> In several cases, the application of the method aims to generate high-energy rare conformers otherwise inaccessible to experiment.<sup>[2–6,8–12]</sup>

A conformational isomerisation occurs when enough energy is deposited into the reaction coordinate, so that the system can overcome the energy barrier and pass into the products valley. The reaction coordinate for internal rotation around a single bond connecting two conformers is essentially described by the torsion about that bond. In

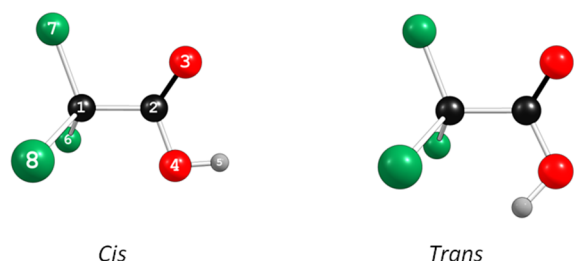


**Figure 1.** Conformers of trichloroacetic acid, with atom numbering.

general, its direct excitation above the barrier is not feasible because its absorption cross section is very low. Alternatively, energy is introduced in the molecule by excitation of a different higher-energy vibration with appreciable absorption cross section.<sup>[2–12]</sup> This energy is then partially transferred to the reaction coordinate through a cascade relaxation mechanism involving participation of matrix phonons.

The paradigmatic systems studied by this approach are carboxylic acids, because the COOH group has two minimum energy conformations which can be interconverted very effectively by excitation of the corresponding OH stretching mode.<sup>[2–4,7–11]</sup> Formic and acetic acids have been studied in detail in various matrix-media.<sup>[2–4,7,9,13–16]</sup> Together with additional studies on other molecules, these investigations allowed to reach some general conclusions: *i*) in general, once formed, the high-energy conformer of the carboxylic acids convert back spontaneously to the more stable form by tunnelling, even at cryogenic temperatures, in time scales that vary from a few seconds to several hours;<sup>[7,8,13–16]</sup> *ii*) the stability of the higher-energy forms depends upon several factors, the dominant one appearing to be the height/wideness of the energy barrier separating the higher energy form from the lower energy one;<sup>[3,7,14]</sup> *iii*) specific interactions with the matrix material affect also the stability of the higher-energy form, which has been found to be greater in solid N<sub>2</sub> and CO<sub>2</sub> than in rare gases;<sup>[7,8,14,15]</sup> *iv*) differences in the matrix microenvironments also influence the life-time of the higher-energy conformer, even if they appear spectroscopically indistinguishable, leading to decay rates that very often obey to a dispersive-type kinetics instead of following a single exponential behaviour.<sup>[5–12]</sup>

The present study focuses on trichloroacetic acid (Cl<sub>3</sub>CCOOH; TCA), which differs from acetic acid by replacement of the methyl group by the strongly electron-attractor trichloromethyl moiety. Such structural modification can be expected to lead to a reduction of the double bond character of the carboxylic C–O bond, implying a lower energy barrier for the *trans* → *cis* conformational isomerization in

TCA, and reducing the stability of the higher-energy *trans* conformer (O=C–O–H dihedral angle: 180°; see Figure 1) once it is generated in a suitable matrix media using the strategy presented above. As described in detail in the next sections, monomers of TCA were isolated in a nitrogen matrix (15 K) and the higher-energy *trans* conformer was generated *in situ* by narrowband near-infrared selective excitation the 1<sup>st</sup> OH stretching overtone of the lower-energy *cis* conformer. Subsequently, the spontaneous *trans*-TCA → *cis*-TCA decay was investigated and compared with data previously obtained for acetic and formic acids.<sup>[2,7,14]</sup> The experimental results were enlightened by the comprehensive characterization of the potential energy surface of the molecule and the detailed assignment of the infrared spectra of the two conformers undertaken by quantum chemistry calculations. This is the first reported doubtless experimental observation of the *trans*-TCA conformer hitherto.

## 2. EXPERIMENTAL AND COMPUTATIONAL METHODS

Trichloroacetic acid was obtained from Sigma, purity > 99 %. Before use, the compound was dried by the standard freeze-pump-thaw method. For matrix preparation, the solid sample was placed in a specially designed Knudsen cell with shut-off possibility and its vapors (at room temperature) were co-deposited with a large excess of the matrix gas (N<sub>2</sub>; 99.999 %) onto the cold CsI substrate (T = 15 K) of the cryostat (APD Cryogenics DE-202A closed-cycle helium refrigerator).

The infrared spectra were recorded, with 0.5 cm<sup>-1</sup> spectral resolution, in a Thermo Nicolet™ 6700 Fourier transform infrared spectrometer, equipped with a deuterated triglycine sulphate (DTGS) detector and a KBr beam splitter for studies in the mid-infrared range and with a CaF<sub>2</sub> beam splitter and an InGaAs detector for near-infrared. The sample compartment of the spectrometer was modified in order to accommodate the cryostat head and allow purging of the instrument by a stream of dry, CO<sub>2</sub> exempted air.

Vibrational excitation of the low-energy conformer of TCA initially present in the matrices was undertaken *in situ*, through the KBr windows of the cryostat, using the idle beam of the Spectra Physics Quanta-Ray® optical parametric oscillator (MOPO-SL) pumped by a Nd:YAG laser (Spectra Physics Quanta-Ray® PRO-230-10). The near-infrared beam has a bandwidth of ~0.2 cm<sup>-1</sup>, pulse frequency of 10 Hz and energy of ~10 mJ.

The quantum chemical calculations were performed using the Gaussian 09 program package<sup>[17]</sup> at the DFT level of theory, using the Dunning's correlation consistent cc-PVDZ basis set<sup>[18,19]</sup> and the three-parameter hybrid density

functional abbreviated as B3LYP.<sup>[20–22]</sup> Relaxed potential energy scans were performed at the same level of theory, and the transition state structure for the *trans*-TCA ↔ *cis*-TCA isomerization located using the synchronous transit-guided quasi-Newton (STQN) method.<sup>[23,24]</sup> The B3LYP/cc-PVDZ calculated vibrational frequencies and infrared intensities were used to assist the analysis of the experimental spectra. The computed harmonic wavenumbers were corrected by applying the simple linear transformation  $\nu_{\text{corr}} = 0.932 \nu_{\text{calc}} + 67.5 \text{ cm}^{-1}$ , which was obtained by fitting the calculated wavenumbers to the experimentally observed infrared bands of both *cis*-TCA and *trans*-TCA conformers. This correction accounts mainly for the effects of basis set limitations, neglected part of electron correlation and anharmonicity effects. Normal coordinate analysis was undertaken in the symmetry internal coordinates space, according to the recommendations of Pulay *et al.*,<sup>[25]</sup> as described by Schachtschneider and Mortimer,<sup>[26]</sup> using the optimized geometries and harmonic force constants resulting from the DFT(B3LYP)/cc-PVDZ calculations. For the purpose of modeling infrared spectra, the calculated frequencies, together with the calculated infrared intensities, served to simulate the spectra shown in the figures by convoluting each peak with a Lorentzian function with a full-width-at-half-maximum of  $2 \text{ cm}^{-1}$ .

### 3. RESULTS AND DISCUSSION

#### 3.1 Potential Energy Landscape of TCA

Trichloroacetic acid is a structurally simple compound, which receives substantial uses, in particular as protein precipitant in clinical chemistry<sup>[27]</sup> and as a caustic for removing wart.<sup>[28–32]</sup> Nevertheless, its structure and vibrational spectra have been very scarcely addressed. A molecular mechanics and vibrational spectroscopy study has been reported by Fausto and Teixeira-Dias, almost 20 years ago,<sup>[33]</sup> where the infrared and Raman spectra of TCA in the crystalline and liquid states were assigned and the calculated structures for the two conformers of the compound, as isolated species, were predicted. The two calculated minima correspond to the *cis* and *trans* conformers about the carboxylic C–O bond, both forms showing the trichloromethyl group oriented in such a way that one of the chlorine atoms eclipses the carbonyl oxygen atom. The molecular mechanics calculations predicted the *cis* form more stable than the *trans* conformer by  $36.2 \text{ kJ mol}^{-1}$ , with a *cis* → *trans* energy barrier of  $51.8 \text{ kJ mol}^{-1}$ . As it will be shown below, these values are both overestimated, in particular that for the energy difference between the conformers. The barrier for internal rotation of the trichloromethyl group in the *cis* conformer was also estimated and a value of  $3.4 \text{ kJ mol}^{-1}$

suggested, which is somewhat lower than that resulting from the calculations carried out in the present study, as described in detail below. The infrared spectrum of anhydrous solid TCA was addressed by Adams and Kim,<sup>[34]</sup> in an attempt to correlate this spectrum with a former structural study of the compound by neutron diffraction.<sup>[35]</sup> TCA was also investigated before theoretically (using the old CNDO/2 semi-empirical method) and in gas phase (by infrared spectroscopy) by Panichkina, Bilobrov and Titov.<sup>[36]</sup> In that study, the *cis* → *trans* energy barrier was calculated as  $\sim 20 \text{ kJ mol}^{-1}$ , and the *trans* conformer suggested to have its trichloromethyl group oriented the opposite way as compared to that in the *cis* conformer, *i.e.*, exhibiting one of the chlorine atoms eclipsed with the acid oxygen atom. The CNDO/2 estimated energy difference between the two conformers was  $\sim 2.5 \text{ kJ mol}^{-1}$ .<sup>[36]</sup> As shown below, the CNDO/2 predicted geometry for the *trans*-TCA conformer as well as both the *trans* – *cis* energy difference and *cis* → *trans* energy barrier are incorrect.

In the present study, the potential energy surface of TCA was investigated at the DFT(B3LYP)/cc-PVDZ level of theory. The calculations reveal that both *cis*- and *trans*-TCA conformers have the trichloromethyl group in the same orientation with respect to the acid group, with one of the chlorine atoms eclipsing the carbonyl oxygen atom (see Figure 1). Both structures exhibit a plane of symmetry, belonging to the  $C_s$  point group. The optimized geometrical parameters for the optimized structures of the two conformers are provided in the Supporting Information Table S1. The potential energy profiles for internal rotation about the C–O bond, interconverting the conformers into each other, and those corresponding to rotation of the trichloromethyl group in the two conformers are shown in Figure 2. The B3LYP/cc-PVDZ calculations predict the energy of the *cis* conformer to be lower than that of the *trans* conformer by  $10.74 \text{ kJ mol}^{-1}$  ( $9.82 \text{ kJ mol}^{-1}$  after inclusion of the zero-point correction), and a *cis* → *trans* energy barrier of  $41.7 \text{ kJ mol}^{-1}$  ( $31.0 \text{ kJ mol}^{-1}$  in the reverse direction). Noteworthy, at room temperature ( $298.15 \text{ K}$ ) the Gibbs energy difference between the conformers was estimated by the calculations as being only  $5.38 \text{ kJ mol}^{-1}$ , suggesting that entropic effects stabilize considerably the *trans* conformer. This result is in agreement with the very low C–C torsional frequency calculated for the *trans*-TCA conformer (predicted as low as  $6.2 \text{ cm}^{-1}$ , that shall be compared with a frequency of  $37.4 \text{ cm}^{-1}$  for the same mode in the *cis* conformer), which demonstrates that in this conformer the internal rotation of the trichloromethyl group corresponds to a large amplitude motion, providing the molecule additional conformational flexibility and increasing its entropy (the calculations predict an increase of *ca.* 5 % in entropy in going from *cis*- to *trans*-TCA).

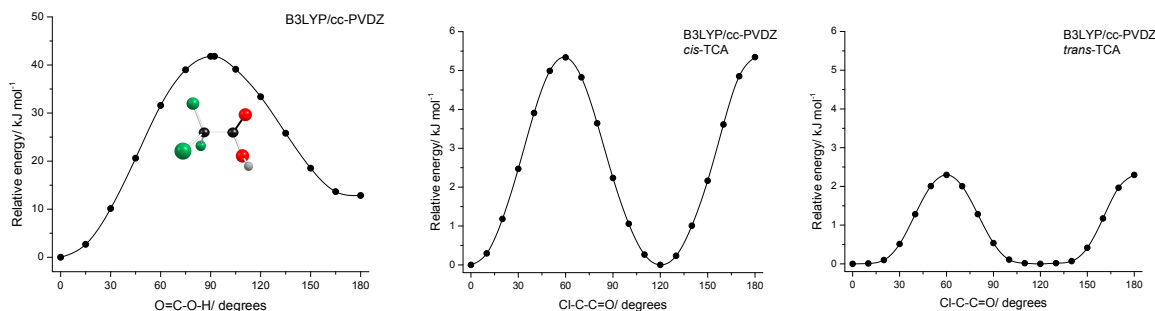


**Figure 2.** B3LYP/cc-PVDZ calculated potential energy profiles for internal rotations about the C–O (*left*) and C–C (*middle and right*) bonds in trichloroacetic acid. The first graph corresponds to the isomerization coordinate and the two last plots to the internal rotation of the  $\text{CCl}_3$  group in the *cis*- and *trans*-TCA conformers, respectively. The inserted structure corresponds to the transition state between the two conformers.

In the transition state for conformational isomerization (see Figure 2), the hydrogen atom is almost perpendicularly oriented in relation to the  $\text{CC}(=\text{O})\text{O}$  plane ( $\text{O}=\text{C}-\text{O}-\text{H}$  dihedral:  $91.3^\circ$ ). The transition states for internal rotation of the trichloromethyl group correspond to the  $C_s$  symmetry structures bearing one of the chlorine atoms eclipsing the acid oxygen atom, defining 3-fold energy barriers of  $5.34$  and  $2.30$   $\text{kJ mol}^{-1}$  in *cis*- and *trans*-TCA, respectively. As expected, the energy barrier in the *trans* conformer is significantly lower than in the *cis* form, mostly due to the steric hindrance in the minimum energy *trans* structure resulting from the proximity of the OH and trichloromethyl groups.

### 3.2 Infrared Spectrum of TCA Isolated in $\text{N}_2$ matrix (15 K)

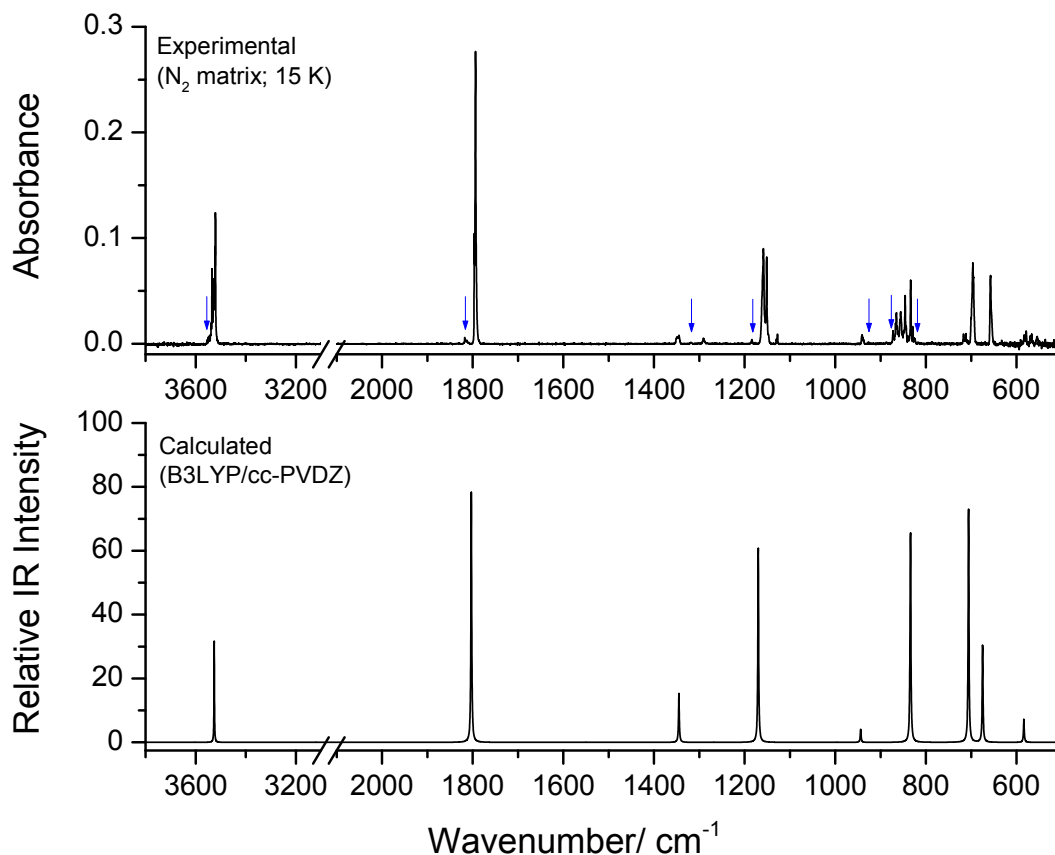
During the deposition of the matrices, the gaseous TCA:argon beam (in  $\sim 1:1000$  ratio) being deposited was kept at room temperature ( $\text{RT} = 298.15$  K), while the temperature of the cold CsI substrate of the cryostat was 15 K. The predicted populations of the *cis*- and *trans*-TCA conformers in the gas phase equilibrium at RT, based on their calculated Gibbs energy difference ( $5.38$   $\text{kJ mol}^{-1}$ ), are 90 % and 10 %, respectively. As already mentioned, the results of the present calculations differ considerably from those previously reported,<sup>[33,36]</sup> obtained at lower theoretical levels, where the relative energy of the two conformers was predicted to be either much higher ( $36.2$   $\text{kJ mol}^{-1}$ ),<sup>[33]</sup> suggesting a negligible population of the *trans*-TCA conformer in the RT gas phase, or much smaller ( $\sim 2.5$   $\text{kJ mol}^{-1}$ ),<sup>[36]</sup> so that the population of the *trans* conformer should be expected to be about 25 %.

Figure 3 shows the infrared spectrum of the as-deposited TCA  $\text{N}_2$ -matrix. The experimental spectrum is compared with the calculated spectrum of the *cis* conformer. It is clear from this Figure that the experimental spectrum is nicely reproduced by the calculated one, indicating that it

contains essentially the vibrational signature of the most stable *cis*-TCA conformer. Nevertheless, low intensity bands are also observed that have no counterparts in the theoretical spectra of *cis*-TCA and that are ascribable to the *trans* conformer. Examples of these bands are the doublets at  $1817.5/1813.1$  and  $1318.2/1291.0$   $\text{cm}^{-1}$  and the multiplet at  $\sim 926$   $\text{cm}^{-1}$ , which fit well some of the most intense predicted infrared bands of *trans*-TCA ( $\nu\text{C}=\text{O}$ :  $1835.1$   $\text{cm}^{-1}$ ;  $\delta\text{COH}$ :  $1311.0$   $\text{cm}^{-1}$ ;  $\nu\text{C}-\text{C}$ :  $926.7$   $\text{cm}^{-1}$ ). The full identification of the vibrational signature of the *trans* conformer has been facilitated by the near-infrared irradiation experiments described in the next section. However, the observation of the bands of this conformer in the spectrum of the as-deposited matrices is in agreement with the presence of this form in the RT gaseous beam used to prepare the samples. In that sense, the present results are in agreement with the previous suggestion by Panichkina, Bilobrov and Titov,<sup>[36]</sup> who have interpreted the observed  $\nu\text{C}=\text{O}$  splitting in the gas phase infrared spectrum of TCA as due to the presence of two conformers of the compound (though as mentioned above they failed in assigning the right structure of the higher energy *trans*-TCA conformer), and also with some previous studies on the compound in diluted  $\text{CCl}_4$  solutions.<sup>[37,38]</sup> It shall also be pointed out here, however, that until now the suggested experimental detection of the *trans*-TCA conformer has been rather controversial.<sup>[36,39]</sup>

Taking into account the calculated relative intensities of the infrared bands of the two conformers, the populations of *cis*- and *trans*-TCA present in the spectrum of the as-deposited  $\text{N}_2$  matrices, estimated from the observed intensities, are *ca.* 95 % and 5 %, respectively. Compared to the predicted relative populations (90 % vs. 10 %) these values are shifted towards the most stable *cis* conformer. The reason for such population shift will be presented in Section 3.4.

Another characteristics of the infrared spectrum of matrix isolated TCA is that several bands exhibit a multiplet



**Figure 3.** Infrared spectrum of TCA isolated in  $N_2$  matrix at 15 K (*top*) and B3LYP/cc-PVDZ calculated infrared spectrum of *cis*-TCA (*bottom*). Bands in the calculated spectrum are simulated by a Lorentzian function centered at the calculated (scaled) wavenumber and with a full-width-at-half-band equal to  $2\text{ cm}^{-1}$ , with calculated intensities corresponding to the area under the function. In the experimental spectrum, the most prominent bands due to conformer *trans* are indicated by the arrows.

structure. This multiplet structure appears very clearly in the case of the most intense bands, which are related with vibrations implying a larger variation of the dipole moment and, then, that are more sensitive to the local environment (see Figure 2). The assignment of the spectrum of *cis*-TCA is given in Table 1, where the calculated infrared spectrum of this form is also shown, together with the results of the performed normal coordinate analysis. The definition of the used symmetry coordinates are provided in Table S2 (Supporting Information).

Considering the good agreement between the experimental and calculated spectra, most of the assignments are straightforward. The multiplet observed in the  $\nu\text{OH}$  stretching region (centered at  $\sim 3528\text{ cm}^{-1}$ ) is a good example of a band exhibiting extensive matrix site-splitting. As it could be expected, the average wavenumber of the  $\nu\text{OH}$  stretching vibration in *cis*-TCA is considerably lower than that of the same vibration in *cis*-acetic acid (*cis*-AA) isolated in  $N_2$  ( $\sim 3549\text{ cm}^{-1}$ ),<sup>[14]</sup> due to the considerably stronger acid character of TCA. On the other hand, the  $\nu\text{C}=\text{O}$  stretching

mode is observed at higher frequency in TCA (main bands at  $1796.5$  and  $1793.7\text{ cm}^{-1}$ ) than in acetic acid ( $1779.0$  and  $1775.7\text{ cm}^{-1}$ ).<sup>[14]</sup> This result correlates with the stronger  $\text{C}=\text{O}$  bond in TCA compared with acetic acid ( $120.00$  vs.  $120.87\text{ pm}$ ; B3LYP/cc-PVDZ calculated data). The two modes predominantly related with the  $\nu\text{C}-\text{O}$  and  $\delta\text{COH}$  coordinates are observed in *cis*-TCA at  $1350.1/1344.8\text{ cm}^{-1}$  and in the  $1162\text{--}1151\text{ cm}^{-1}$  range, the lower wavenumber mode having a larger contribution from the  $\nu\text{C}-\text{O}$  coordinate (see Table 1). In *cis*-AA, these modes are observed around  $1285\text{ cm}^{-1}$  and in the  $1206\text{--}1177\text{ cm}^{-1}$  region,<sup>[14]</sup> with the lower frequency mode absorbing at slightly higher values in relation TCA in agreement with the expectations. The  $\nu\text{C}-\text{C}$  vibration is observed in *cis*-TCA around  $940\text{ cm}^{-1}$  and in *cis*-AA near  $855\text{ cm}^{-1}$ .<sup>[14]</sup> Since the  $\text{C}-\text{C}$  bond is longer in TCA than in acetic acid ( $155.70$  vs.  $150.72\text{ pm}$ ; B3LYP/cc-PVDZ calculated values), the larger  $\nu\text{C}-\text{C}$  stretching frequency in *cis*-TCA is an indication that the elongation of the  $\text{C}-\text{C}$  bond in TCA results mostly from through-space repulsion between the negatively charged substituents at the

**Table 1.** Assignment of the observed infrared spectrum (3600–450  $\text{cm}^{-1}$  range) of *cis*-TCA conformer, and B3LYP/cc-PVDZ calculated infrared wavenumbers and infrared intensities and results of normal coordinate analysis for this conformer.<sup>(a)</sup>

Observed $\nu/\text{cm}^{-1}$	Calculated <sup>(b)</sup>		Approximate description	PED <sup>(c)</sup> / %
	$\nu/\text{cm}^{-1}$	$I^{\text{R}}/\text{km mol}^{-1}$		
3534.8/3530.6sh/3529.4/3526.6sh/3525.9/3522.6/3521.0	3525.6	99.7	$\nu\text{OH}$	$A'$ $S_1(100)$
1796.5/1795.9sh/1794.6sh/1793.7	1802.6	246.5	$\nu\text{C}=\text{O}$	$A'$ $S_2(89)$
1350.1/1344.8	1345.0	48.3	$\delta\text{COH}$ , $\nu\text{C}-\text{O}$	$A'$ $S_8(44) + S_3(28) + S_9(16)$
1162.0/1160.4sh/1158.6/1155.9sh/1151.2/1149.8sh/1147.5	1170.0	191.2	$\nu\text{C}-\text{O}$ , $\delta\text{COH}$	$A'$ $S_8(43) + S_3(41)$
941.6/940.8/939.2/937.3	943.6	12.9	$\nu\text{CC}$	$A'$ $S_4(48) + S_3(17) + S_{13}(17) + S_7(13)$
868–832 <sup>(d)</sup> with main maxima at: 865.1/855.9 and at: 845.9/833.7	834.9 834.1	38.9 186.2	$\gamma\text{C}=\text{O}$ $\nu\text{CCl}_3 \text{ as}'$	$A''$ $S_{14}(53) + S_{16}(20) + S_6(15)$ $A'$ $S_5(53) + S_{10}(16) + S_{15}(15) + S_{11}(11)$
700.5/699.1sh/697.5sh/696.5/695.7sh/694.9/692.8sh	706.4	229.4	$\nu\text{CCl}_3 \text{ as}''$	$A''$ $S_6(53) + S_{17}(32) + S_{14}(11)$
658.2/657.3	674.5	95.4	$\delta\text{OCO}$	$A'$ $S_9(61) + S_7(10)$
591.1/583.4/579.0/569.8/566.9/554.6	584.1	22.8	$\tau\text{COH}$	$A''$ $S_{17}(64) + S_{14}(19) + S_6(17)$
not observed	464.3	1.7	$\nu\text{CCl}_3 \text{ s}$	$A'$ $S_7(77) + S_4(14)$
not observed	452.6	0.6	$\delta\text{CCO}$	$A'$ $S_{10}(39) + S_5(34) + S_9(10)$

<sup>(a)</sup> Wavenumbers ( $\nu/\text{cm}^{-1}$ ), calculated infrared intensities ( $I^{\text{R}}/\text{km mol}^{-1}$ ).

<sup>(b)</sup> Wavenumbers corrected according to the equation  $\nu_{\text{corr}} = 0.932 \nu_{\text{calc}} + 67.5 \text{ cm}^{-1}$ ; for non-corrected wavenumbers (full spectral range) see Table S3 in the Supporting Information.

<sup>(c)</sup> See Table S2 (Supporting Information) for definition of symmetry coordinates; only PED values equal or larger to 10 % are shown.

<sup>(d)</sup> The assignment of specific bands to the  $\gamma\text{C}=\text{O}$  and  $\nu\text{CCl}_3 \text{ as}'$  modes is difficult because the close values of the calculated wavenumbers for the two modes and because experimentally the feature observed in this range shows a complex multiplet structure with a large number of maxima (the proposed assignment of the specified main maxima to one of the modes is tentative).

carbon atoms forming the bond (the three chlorine atoms at one carbon and the two oxygen atoms at the second one), while the polarization of the C–C bond is smaller, leading to an effective larger electron density of the bond. Also, the two bending modes associated with the carboxylic group,  $\gamma\text{C}=\text{O}$  and  $\delta\text{OCO}$ , give rise to bands appearing at higher wavenumbers in *cis*-CA (in the 865–855  $\text{cm}^{-1}$  range and at 658.2/657.3  $\text{cm}^{-1}$ ) than in *cis*-AA (in the 554–550 and 588–585  $\text{cm}^{-1}$  ranges, respectively). These shifts to higher wavenumbers in TCA result mainly from the coupling of the  $\gamma\text{C}=\text{O}$  and  $\delta\text{OCO}$  coordinates with the  $\nu\text{CCl}_3$  stretching coordinates (see Table 1). On the other hand, the  $\tau\text{COH}$  torsion appears at lower frequency in *cis*-TCA (as a multiplet between 591.1 and 554.6  $\text{cm}^{-1}$ ) than in *cis*-AA (between 663.2 and 654.6  $\text{cm}^{-1}$ ),<sup>[14]</sup> because of the considerably shallow torsional potential in TCA compared to acetic acid (see previous section), which implies a lower torsional force constant in the presently studied molecule.

The stretching vibrations of the trichloromethyl group for *cis*-TCA are predicted at 834.1, 706.4 (anti-symmetric modes) and 464.3  $\text{cm}^{-1}$  (symmetric mode). The anti-symmetric modes are observed around 850 and 700  $\text{cm}^{-1}$ , in good agreement with the theoretical values, while the symmetric vibration is of very low intensity (1.7  $\text{km mol}^{-1}$ ; see Table 1) and could not be observed (this is mainly due to the fact that below 500  $\text{cm}^{-1}$  the registered spectra show a higher noise, since the spectrometer beam has to go through the two external KBr windows of the cryostat, plus

the CsI of the cold substrate, which considerably reduces transmittance in this spectral region). The observed  $\nu\text{CCl}_3$  anti-symmetric stretching modes give rise to extensively splitted bands (see Table 1). We have performed vibrational calculations on all  $^{35}\text{Cl}/^{37}\text{Cl}$  isotopologues of the compound and found out that the maximum frequency shifts due to different chlorine isotopic substitution are smaller than 2  $\text{cm}^{-1}$  for both  $\nu\text{CCl}_3$  anti-symmetric stretching modes (9  $\text{cm}^{-1}$  in the case of the non-observed  $\nu\text{CCl}_3$  symmetric stretching mode). Hence, the extensive splitting observed for bands due to the  $\nu\text{CCl}_3$  anti-symmetric stretching vibrations (which spread over more than 10 and 5  $\text{cm}^{-1}$  for the  $A'$  and  $A''$  symmetry modes, respectively; see Table 1) cannot be ascribed to the co-existence of different isotopologues of the molecule, and shall be ascribed mostly to matrix-site effects (in the case of the  $A''$  mode, reinforced by an extensive coupling with the  $\tau\text{COH}$  torsional coordinate; Table 1).

### 3.3 Narrowband NIR-Induced Generation of *trans*-TCA

Near-infrared radiation, tuned at the frequency of the first  $\nu\text{OH}$  overtone of *cis*-TCA, was used to vibrationally excite this conformer. In the near-infrared range, the band corresponding to the  $2\nu\text{OH}$  overtone of *cis*-TCA is observed between 6905.4 and 6897.1  $\text{cm}^{-1}$ , with maximum at 6898.5  $\text{cm}^{-1}$ . Irradiation of the matrix isolated *cis*-TCA at this latter wavenumber resulted in its conversion into the

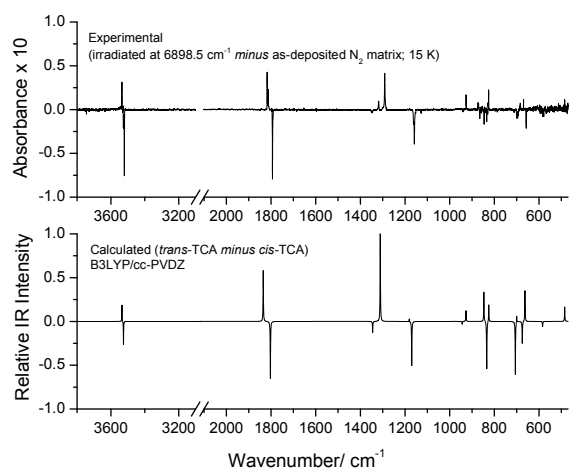


**Figure 4.** Infrared difference spectrum obtained by subtracting the spectrum of the as-deposited TCA  $N_2$ -matrix from the spectrum obtained after near-infrared irradiation at  $6898.5\text{ cm}^{-1}$  ( $2\nu\text{OH}$  *cis*-TCA) during 45 min. (*top*) and simulated difference spectrum built based on the B3LYP/cc-PVDZ calculated infrared spectra of *trans*-TCA (bands pointing up) and *cis*-TCA (bands pointing down) (*bottom*). Bands in the calculated spectrum are simulated by a Lorentzian function centered at the calculated (scaled) wavenumber and with a full-width-at-half-band equal to  $2\text{ cm}^{-1}$ , with calculated intensities corresponding to the area under the function; the calculated difference spectrum was normalized to the most intense band.

higher-energy *trans* conformer. The results are summarized in Figure 4, where the difference spectrum (spectrum obtained after irradiation at  $6898.5\text{ cm}^{-1}$  during 45 min. *minus* spectrum of the as-deposited matrix) is compared with the simulated difference spectrum (*trans*-TCA *minus cis*-TCA) obtained from the B3LYP/cc-PVDZ calculations. The occurrence of the isomerization reaction is doubtless, with the emerging spectrum fitting very well the calculated one for the *trans* conformer. Assignments for this form are given in Table 2, where the results of the performed normal coordinate analysis are also presented. Following the general trend,<sup>[2,3,8,14]</sup> both the  $\nu\text{OH}$  and  $\nu\text{C}=\text{O}$  stretching vibrations in *trans*-TCA appear shifted to higher frequencies when compared to those of the *cis*-TCA form. The average shifts are both *ca.*  $20\text{ cm}^{-1}$ , what contrasts with what was found in acetic acid, where the corresponding  $\nu\text{OH}$  and  $\nu\text{C}=\text{O}$  shifts are of *ca.*  $60$  and  $20\text{ cm}^{-1}$ , respectively. The smaller  $\nu\text{OH}$  shift observed for TCA results from the fact that in this molecule the OH group is oriented towards electronegative groups in both conformers, whereas in acetic acid it is oriented towards an electronegative one in the case of the *cis* form but points to the electropositive methyl group in the *trans* conformer. The different prevalent charges in the two conformers of acetic acid in the vicinity of the OH group lead to considerably diverse polarization-induced changes in the OH bond of the two conformers, thus making their associated  $\nu\text{OH}$  vibrational frequencies considerably more dissimilar than in the two TCA forms.

**Table 2.** Assignment of the observed infrared spectrum ( $3600\text{--}450\text{ cm}^{-1}$  range) of *trans*-TCA conformer, and B3LYP/cc-PVDZ calculated infrared wavenumbers and infrared intensities and results of normal coordinate analysis for this conformer.<sup>(a)</sup>

Observed $\nu/\text{cm}^{-1}$	Calculated <sup>(b)</sup> $\nu/\text{cm}^{-1}$	$I^{\text{IR}}/\text{km mol}^{-1}$	Approximate description	PED <sup>(c)</sup> /%
3553.3/3549.8/3545.1/3544.0sh/3540.8/3538.0/3534.8	3534.8	71.1	$\nu\text{OH}$	$A'$ $S_1(100)$
1817.5/1816.2sh/1813.9sh/1813.1	1835.1	220.8	$\nu\text{C}=\text{O}$	$A'$ $S_2(88)$
1318.2/1300.3/1291.0/1288.5sh/1283.0 <sup>(d)</sup>	1311.0	377.4	$\delta\text{COH}$	$A'$ $S_8(64) + S_3(19)$
1187.4/1180.2/1178.2	1181.3	11.8	$\nu\text{C}-\text{O}$	$A'$ $S_3(51) + S_8(29)$
926.8/925.5/924.9/923.9	926.7	46.8	$\nu\text{CC}$	$A'$ $S_4(46) + S_3(15) + S_{13}(15) + S_7(13)$
872.8/871.4/870.7	846.6	128.5	$\nu\text{CCl}_3\text{ as}'$	$A'$ $S_5(49) + S_{10}(15) + S_{15}(14)$
828.5/825.6	825.4	74.3	$\gamma\text{C}=\text{O}$	$A''$ $S_{14}(52) + S_{16}(20) + S_6(13)$
685.4/684.1	700.0	29.3	$\delta\text{OCO}$	$A'$ $S_9(66) + S_7(10)$
669.5	663.2	133.7	$\nu\text{CCl}_3\text{ as}''$	$A''$ $S_6(68) + S_{14}(23)$
484.8	484.8	62.1	$\tau\text{COH}$	$A''$ $S_{17}(87) + S_{14}(10)$
not observed	461.2	8.9	$\nu\text{CCl}_3\text{ s}$	$A'$ $S_7(39) + S_9(15) + S_5(15) + S_{10}(12)$
not observed	455.4	12.4	$\delta\text{CCO}, \nu\text{CCl}_3\text{ s}$	$A'$ $S_7(35) + S_{10}(28) + S_5(22)$

<sup>(a)</sup> Wavenumbers ( $\nu/\text{cm}^{-1}$ ), calculated infrared intensities ( $I^{\text{IR}}/\text{km mol}^{-1}$ ).

<sup>(b)</sup> Wavenumbers corrected according to the equation  $\nu_{\text{corr}} = 0.932 \nu_{\text{calc}} + 67.5\text{ cm}^{-1}$ ; for non-corrected wavenumbers (full spectral range) see Table S3 in the Supporting Information.

<sup>(c)</sup> See Table S2 (Supporting Information) for definition of symmetry coordinates; only PED values equal or larger to 10% are shown.

<sup>(d)</sup> Fermi resonance with the combination tone  $\tau\text{COH} + \gamma\text{C}=\text{O}$ .

The situation is distinct in the case of the carbonyl group, which shows identical vicinities in the analogous conformers of the two molecules.

An interesting observation is that in *trans*-TCA the degree of mixing of the  $\nu\text{C}=\text{O}$  and  $\delta\text{COH}$  coordinates in the two vibrations with predominant contributions from these oscillators is much smaller than in *cis*-TCA, with the higher-frequency mode having a dominant contribution from  $\delta\text{COH}$  and the lower frequency one a major contribution from  $\nu\text{C}=\text{O}$  (see Table 2). This trend has already been noticed in the case of acetic acid.<sup>[14]</sup> Also as in *trans*-AA, the  $\delta\text{COH}$  mode in *trans*-TCA is involved in a Fermi resonance interaction with a combination tone ( $\tau\text{COH} + \nu\text{C}=\text{O}$ ), thus appearing as a characteristic Fermi doublet around 1318.2 and 1291.0  $\text{cm}^{-1}$  (with some low-intensity satellite bands due to matrix-site splitting).

The relative frequencies of the  $\nu\text{C}=\text{C}$  mode in *trans* and *cis*-TCA ( $\sim 925$  vs.  $940$   $\text{cm}^{-1}$ , respectively) correlate well with the corresponding B3LYP/cc-PVDZ calculated bond lengths (156.87 and 155.70 pm, respectively). The  $\nu\text{C}=\text{O}$  vibration is observed at nearly the same frequency in both conformers. On the other hand, the  $\delta\text{OCO}$  bending mode increases its frequency by *ca.*  $30$   $\text{cm}^{-1}$  (see Tables 1 and 2) when going from *cis*-TCA to *trans*-TCA. Such shift is much probably determined by the significant changes in the angles of the  $\text{C}(=\text{O})\text{O}$  fragment upon isomerization ( $\text{O}=\text{C}-\text{O}/\text{C}=\text{O}/\text{C}-\text{O}$ :  $125.48/124.07/110.45^\circ$  in *cis*-TCA, vs.  $123.02/122.42/114.56^\circ$  in *trans*-TCA; see Table S1). Finally, as expected taking into account the much flat potential associated with the torsion around the  $\text{C}-\text{O}$  bond in the vicinity of the *trans* conformation (see Figure 2), the  $\tau\text{COH}$  torsion absorbs at much lower frequency in the *trans*-TCA conformer ( $484.8$   $\text{cm}^{-1}$ ) than in the *cis*-TCA form (between  $591.1$  and  $554.6$   $\text{cm}^{-1}$ ).

An additional note shall be made in relation to the stretching vibrations of the trichloromethyl group. While the  $A'$  symmetry  $\nu\text{CCl}_3$  anti-symmetric stretching is observed at nearly the same frequency in both conformers of TCA, the  $A''$  mode absorbs at a significantly lower frequency in the *trans*-TCA conformer ( $669.5$   $\text{cm}^{-1}$ , vs. about  $700$   $\text{cm}^{-1}$  in the *cis* conformer). Also, interestingly, this mode gives rise to an essentially single band in the *trans* conformer, while in the *cis* form it is observed as a complex multiplet of bands. The fact that the vibration is substantially coupled with the  $\tau\text{COH}$  torsional coordinate in *cis*-TCA while it does not mix with this coordinate in the *trans* conformer may be in the origin of these observations.

### 3.4 *Trans*-TCA $\rightarrow$ *cis*-TCA Spontaneous Decay, by Tunneling

Once the higher-energy *trans*-TCA conformer has been produced by vibrational excitation of the *cis* conformer, the matrix was kept in the dark and its evolution with time was

monitored by recording its mid-infrared spectra periodically. As found for other carboxylic acids<sup>[2,3,7-10,13-15]</sup> (and also other molecules bearing the OH fragment)<sup>[5,6,11,12]</sup> spontaneous conversion of *trans*-TCA into *cis*-TCA, by tunneling, was observed, as noticed by the decrease of intensity of the bands ascribed to *trans*-TCA and simultaneous recover of bands due to the *cis* form. Figure 5 shows the evolution with time of the intensity of the  $\nu\text{C}=\text{O}$  stretching band of *trans*-TCA ( $1818\text{--}1812$   $\text{cm}^{-1}$  range), where the intensity of the band in the last spectrum resulting from near-IR irradiation at  $6898.5$   $\text{cm}^{-1}$  was normalized to unity. The decay curve could be fitted by a stretching exponential function (see legend of Figure 5), indicating that the decay obeys a dispersive type kinetics, as found frequently for this type of processes,<sup>[12]</sup> and showing that the morphology of the different matrix sites affects the decay rate of individual molecules.

The time required for reduction to half of the population initially generated of the *trans*-TCA conformer was  $\sim 720$  s, which is substantially lower than those observed previously for both acetic and formic acids in  $\text{N}_2$  matrix ( $\sim 5$  h and *ca.* 7 h, respectively).<sup>[14]</sup> The faster decay of *trans*-AA compared to *trans*-FA has been explained<sup>[14]</sup> by the lower *trans* $\rightarrow$ *cis* barrier in acetic acid ( $32.9$  vs.  $38.5$   $\text{kJ mol}^{-1}$  in formic acid; B3LYP/cc-PVDZ calculated values). Indeed, the barrier height seems to be the most important factor controlling the tunneling rate, though other factors, like

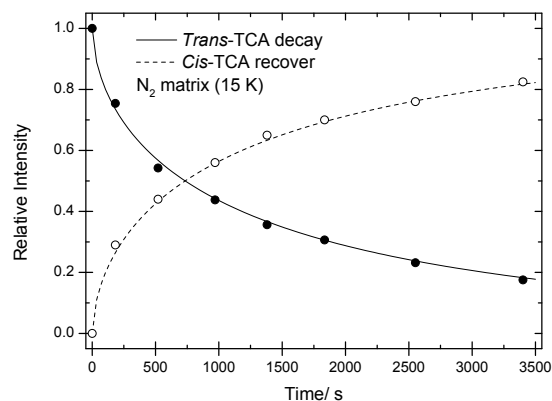


**Figure 5.** Decay of *trans*-TCA into *cis*-TCA in a nitrogen matrix at 15 K. The  $\nu\text{C}=\text{O}$  stretching bands of *trans*- and *cis*-TCA bands in the  $1818\text{--}1812$  and  $1800\text{--}1785$   $\text{cm}^{-1}$  ranges were used to follow the *trans* $\rightarrow$ *cis* conversion. The fitting decay curve obeys to a dispersive type kinetics,  $y = \exp(-at^b)$ , with  $a = 0.0146 \pm 0.0024$  and  $b = 0.585 \pm 0.022$ ;  $R^2 = 0.9968$ ; the recovering curve for *cis*-TCA obeys the equation  $y = [1 - \exp(-at^b)]$ , with  $a$  and  $b$  parameters made equal to those fitted to the decay curve of the *trans* conformer; the relative intensities for *cis*-TCA were normalized in order to have the last point equal to the difference between the unity and the relative intensity of *trans*-TCA.

nature and distribution of the vibrational energy levels involved in the tunneling process, may also play a role in determining the kinetics of the process.<sup>[14,40–42]</sup> The present B3LYP/cc-PVDZ calculations estimated the *trans*→*cis* barrier in TCA as being 31.0 kJ mol<sup>-1</sup>, *i.e.*, lower than those for acetic and formic acids. Accordingly, the observed decay of the high-energy conformer of TCA is faster than for both formic and acetic acids by ~35 and *ca.* 25 times, respectively. The present results then give further support to the idea that the size of the barrier is the most relevant factor determining the tunneling decay rate of *trans* carboxylic acid conformers into their lower-energy *cis* counterparts.<sup>[14,40–42]</sup>

The fast decay observed for *trans*-TCA does also justify two additional observations: firstly, the fact that no evidence of trapping of the *trans*-TCA conformer could be found upon deposition of the compound in argon and xenon matrices (it has been shown that the stability of *trans* carboxylic acid conformers in noble gases is much smaller than in N<sub>2</sub>,<sup>[14,40–42]</sup> so that the *trans*-TCA molecules existing in the gas phase equilibrium prior to deposition promptly convert into the more stable *cis* form in these matrices, precluding its spectroscopic detection); secondly, the fact pointed out in Section 3.2 that the population of the *trans*-TCA conformer observed in the as-deposited N<sub>2</sub> matrix was smaller than that predicted by the calculations for the room temperature gas phase equilibrium, since this conformer could also convert partially into the more stable *cis*-TCA form during deposition (the cold substrate local temperature during deposition at the molecules landing point is somewhat higher than 15 K, because the gaseous beam is at a higher temperature and heat dissipation is not instantaneous, thus facilitating the *trans*-TCA to *cis*-TCA conversion; this local heating during deposition of a cryogenic matrix is the main factor responsible for changes in the trapped conformational populations compared to those existing in the gas phase equilibrium prior to deposition in matrix isolation experiments, playing a role even in the cases where the isomerization has to take place *via* the over the barrier mechanism, in cases where the barrier is small, *i.e.*, of a few kJ mol<sup>-1</sup>).<sup>[11,43]</sup>

## 4. CONCLUSIONS

We were able to generate, for the first time, the higher-energy conformer of trichloroacetic acid, through narrow-band selective near-infrared vibrational excitation of the more stable *cis*-TCA conformer, and measure its decay rate in a N<sub>2</sub> cryomatrix, at 15 K. The half-life of the *trans*-TCA conformer in a N<sub>2</sub> matrix at 15 K (~720 s) was found to be shorter than that of both *trans*-AA and *trans*-formic acid under identical experimental conditions by more than one

order of magnitude, in agreement with the lower *trans*→*cis* energy barrier in TCA compared to acetic and formic acids. The experimental studies received support from quantum chemistry calculations undertaken at the DFT(B3LYP)/cc-pVDZ level of approximation, which allowed the first detailed characterization of the potential energy surface of the molecule and the detailed assignment of the infrared spectra of the two conformers.

**Acknowledgements.** The authors thank the Portuguese Science Foundation (FCT), Lisbon, Portugal, for funding the Coimbra Chemistry Centre (FCT project PEst-OE/UI0313/2014, which is supported in part also by FEDER – European Regional Development Fund, through the COMPETE Programme, Operational Programme for Competitiveness). R. R. F. Bento acknowledges the Scholarship from CAPES Foundation (Proc. no. BEX 2010/14-3).

**Supplementary Information.** Supporting information to the paper is enclosed to the electronic version of the article at: <http://dx.doi.org/10.5562/cca2704>. Table S1, with the B3LYP/cc-PVDZ optimized geometrical parameters for *cis* and *trans*-TCA; Table S2, with the definition of the symmetry coordinates used in the normal coordinate analysis performed on both conformers of TCA; Table S3, with the B3LYP/cc-PVDZ calculated infrared spectra for *cis* and *trans*-TCA and results of normal coordinate analysis for both conformers.

## REFERENCES

- [1] R. T. Hall, G. C. Pimentel, *J. Chem. Phys.* **1963**, *38*, 1889.
- [2] M. Pettersson, J. Lundell, L. Khriachtchev, M. Räsänen, *J. Am. Chem. Soc.* **1997**, *119*, 11715.
- [3] E. M. S. Maçôas, L. Khriachtchev, M. Pettersson, R. Fausto, M. Räsänen, *J. Am. Chem. Soc.* **2003**, *125*, 16188.
- [4] E. M. S. Maçôas, R. Fausto, M. Pettersson, L. Khriachtchev, M. Räsänen, *J. Phys. Chem. A* **2000**, *104*, 6956.
- [5] L. Lapinski, M. J. Nowak, I. Reva, H. Rostkowska, R. Fausto, *Phys. Chem. Chem. Phys.* **2010**, *12*, 9615.
- [6] C. M. Nunes, L. Lapinski, R. Fausto, I. Reva, *J. Chem. Phys.* **2013**, *138*, 125101.
- [7] R. Fausto, L. Khriachtchev, P. Hamm, in: *Physics and Chemistry at Low Temperatures*, (Ed.: L. Khriachtchev), World Scientific **2010**, Chap. 3. pp. 51–84.
- [8] N. Kuş, R. Fausto, *J. Chem. Phys.* **2014**, *141*, 234310.
- [9] M. Hakala, K. Marushkevich, L. Khriachtchev, K. Hämäläinen, M. Räsänen, *J. Chem. Phys.* **2011**, *134*, 054506.

- [10] I. Reva, C. M. Nunes, M. Biczysko, R. Fausto, *J. Phys. Chem. A* **2015**, *119*, 2614.
- [11] N. Kuş, A. Sharma, I. Peña, M. C. Bermudez, C. Cabezas, J. L. Alonso, R. Fausto, *J. Chem. Phys.* **2013**, *138*, 144305.
- [12] L. Lapinski, I. Reva, H. Rostkowska, R. Fausto, M. J. Nowak, *J. Phys. Chem. B* **2014**, *118*, 2831.
- [13] E. M. S. Maçôas, J. Lundell, M. Pettersson, L. Khriachtchev, R. Fausto, M. Räsänen, *J. Mol. Spectrosc.* **2003**, *219*, 70.
- [14] S. Lopes, A. V. Domanskaya, R. Fausto, M. Räsänen, L. Khriachtchev, *J. Chem. Phys.* **2010**, *133*, 144507.
- [15] M. Tsuge, K. Marushkevich, M. Räsänen, L. Khriachtchev, *J. Phys. Chem. A* **2012**, *116*, 5305.
- [16] L. O. Paulson, D. T. Anderson, J. Lundell, K. Marushkevich, M. Melavuori, L. Khriachtchev, *J. Phys. Chem. A* **2011**, *115*, 13346.
- [17] M. J. Frisch, G. W. Trucks, H. B. Schlegel, G. E. Scuseria, M. A. Robb, J. R. Cheeseman, G. Scalmani, V. Barone, B. Mennucci, G. A. Petersson, *et al. Gaussian 09, Revision A.02*; Gaussian, Inc.: Wallingford, CT, **2009**.
- [18] T. H. Dunning Jr., *J. Chem. Phys.* **1989**, *90*, 1007.
- [19] G. P. F. Wood, L. Radom, G. A. Petersson, E. C. Barnes, M. J. Frisch, J. A. Montgomery Jr., *J. Chem. Phys.* **2006**, *125*, 094106.
- [20] A. D. Becke, *Phys. Rev. A* **1988**, *38*, 3098.
- [21] C. Lee, W. Yang, R. G. Parr, *Phys. Rev. B* **1988**, *37*, 785.
- [22] S. H. Vosko, L. Wilk, M. Nusair, *Can. J. Phys.* **1980**, *58*, 1200.
- [23] C. Peng, H. B. Schlegel, *Israel J. Chem.* **1993**, *33*, 449.
- [24] C. Peng, P. Y. Ayala, H. B. Schlegel, M. J. Frisch, *J. Comp. Chem* **1996**, *17*, 49.
- [25] P. Pulay, G. Fogarasi, F. Pang, J. E. Boggs, *J. Am. Chem. Soc.* **1979**, *101*, 2550.
- [26] J. H. Schachtschneider, F. S. Mortimer, *Vibrational Analysis of Polyatomic Molecules. VI. FORTRAN IV Programs for Solving the Vibrational Secular Equation and for the Least-Squares Refinement of Force Constants*, Project No. 31450. Structural Interpretation of Spectra; Shell Development Co: Houston, TX, 1965.
- [27] D. Rajalingam, C. Loftis, J. J. Xu, T. K. S. Kumar, *Protein Sci.* **2009**, *18*, 980.
- [28] D. A. Hudson, R. U. Lechtape-Gruter, *S. Afr. Med. J.* **1990**, *78*, 748.
- [29] A. Yug, J. E. Lane, M. S. Howard, D. E. Kent, *Dermatol. Surg.* **2006**, *32*, 985.
- [30] P. S. Collins, The Chemical Peel, *Clin. Dermatol.* **1987**, *5*, 57.
- [31] P. S. Collins, *J. Dermatol. Surg. Oncol.* **1989**, *15*, 933.
- [32] K. R. Beutner, M. V. Reitano, G. A. Richwald, D. J. Wiley, *Clin. Infect. Dis.* **1998**, *27*, 796.
- [33] R. Fausto, J. J. C. Teixeira-Dias, *J. Mol. Struct.* **1986**, *144*, 241.
- [34] J. Adams, H. Kim, *Spectrochim. Acta A* **1973**, *29*, 675.
- [35] P. Jönsson, W. Hamilton, *J. Chem. Phys.* **1972**, *56*, 4433.
- [36] V. A. Panichkina, V. M. Bilobrov, E. V. Titov, *Teoret. Eksperiment. Khim. (Translated)* **1980**, *16*, 133.
- [37] E. V. Titov, V. M. Belobrov, *Voprosy Stereokhimii* **1971**, *1*, 145.
- [38] E. V. Titov, S. I. Chekushin, V. E. Umanskii, V. M. Belobrov, *Dokl. Akad. Nauk USSR B* **1972**, *12*, 1088.
- [39] I. S. Perelygin, A. M. Afanas'eva, *Appearance of Autoassociation of Halosubstituted Monocarboxylic Acids in the Absorption Spectra in the Region of the Stretching Vibrations of the Carbonyl Groups*, in: *Intermolecular Interaction in Condensed Media* [in Russian], Naukova Dumka, Kiev, **1974**, pp. 103–106.
- [40] E. M. S. Maçôas, L. Khriachtchev, M. Pettersson, R. Fausto, M. Räsänen, *Phys. Chem. Chem. Phys.* **2005**, *7*, 743.
- [41] E. M. Maçôas, L. Khriachtchev, M. Pettersson, R. Fausto, M. Räsänen, *J. Chem. Phys.* **2004**, *121*, 1331.
- [42] M. Pettersson, E. M. S. Maçôas, L. Khriachtchev, J. Lundell, R. Fausto, M. Räsänen, *J. Chem. Phys.* **2002**, *117*, 9095.
- [43] I. D. Reva, S. G. Stepanian, L. Adamowicz, R. Fausto, *Chem. Phys. Lett.* **2003**, *374*, 631.

## Supporting Information

### Narrowband NIR-Induced *In Situ* Generation of the High-Energy *Trans* Conformer of Trichloroacetic Acid Isolated in Solid Nitrogen and its Spontaneous Decay by Tunneling to the Low-Energy *Cis* Conformer

R. F. G. Apóstolo,<sup>a</sup> R. R. F. Bento<sup>a,b</sup> and R. Fausto<sup>a,\*</sup>

<sup>a</sup>Department of Chemistry, University of Coimbra, P 3004–535, Coimbra, Portugal

<sup>b</sup>Instituto de Física, Universidade Federal de Mato Grosso, 78060-900, Cuiabá, Brazil

### Contents

<b>Table S1.</b> B3LYP/cc-PVDZ optimized geometric parameters for <i>cis</i> - and <i>trans</i> -TCA. ....	2
<b>Table S2.</b> Definition of the symmetry coordinates used in the normal coordinate analysis of trichloroacetic acid. ....	3
<b>Table S3.</b> B3LYP/cc-PVDZ calculated infrared spectra for <i>cis</i> - and <i>trans</i> -TCA and results of normal coordinate analysis for both conformers. ....	4

---

\*Corresponding author (E-mail: rfausto@ci.uc.pt).

**Table S1** – B3LYP/cc-PVDZ optimized geometric parameters for *cis*- and *trans*-TCA. <sup>a</sup>

Parameter	<i>cis</i> -TCA	<i>trans</i> -TCA	Parameter	<i>cis</i> -TCA	<i>trans</i> -TCA
C=O	120.00	119.45	C–Cl <sub>6,8</sub>	180.36	181.52
C–O	133.96	134.06	C–Cl <sub>7</sub>	178.14	176.92
O–H	97.53	97.27	C–C	155.70	156.87
C–C=O	124.07	122.42	C–C–Cl <sub>6,8</sub>	108.68	108.24
C–C–O	110.45	114.56	C–C–Cl <sub>7</sub>	109.95	111.10
O=C–O	125.48	123.02	Cl <sub>7</sub> –C–Cl <sub>6,8</sub>	109.80	110.19
C–O–H	106.42	110.80	Cl <sub>6</sub> –C–Cl <sub>8</sub>	109.91	108.82
O=C–O–H	0.00	180.00	Cl <sub>7</sub> –C–C=O	0.00	0.00
			Cl <sub>6,8</sub> –C–C=O	±120.36	±121.11

<sup>a</sup> Bond lengths in pm; angles in degrees. See Figure 1 for atom numbering.

**Table S2** – Definition of the symmetry coordinates used in the normal coordinate analysis of trichloroacetic acid. <sup>a</sup>

Coordinate	Sym.	Definition <sup>b</sup>	Approximate Description <sup>c</sup>
S <sub>1</sub>	A´	r(O–H)	vOH
S <sub>2</sub>	A´	r(C=O)	vC=O
S <sub>3</sub>	A´	r(C–O)	vC–O
S <sub>4</sub>	A´	r(C–C)	vCC
S <sub>5</sub>	A´	2r(C–Cl <sub>7</sub> ) – r(C–Cl <sub>6</sub> ) – r(C–Cl <sub>8</sub> )	vCCl <sub>3</sub> as´
S <sub>6</sub>	A´´	r(C–Cl <sub>6</sub> ) – r(C–Cl <sub>8</sub> )	vCCl <sub>3</sub> as´´
S <sub>7</sub>	A´	r(C–Cl <sub>7</sub> ) + r(C–Cl <sub>6</sub> ) + r(C–Cl <sub>8</sub> )	vCCl <sub>3</sub> s
S <sub>8</sub>	A´	α(C–O–H)	δCOH
S <sub>9</sub>	A´	2α(O–C=O) – α(C–C=O) – α(C–C–O)	δOCO
S <sub>10</sub>	A´	α(C–C=O) – α(C–C–O)	δCCO
S <sub>11</sub>	A´	2α(Cl <sub>6</sub> –C–Cl <sub>8</sub> ) – α(Cl <sub>7</sub> –C–Cl <sub>6</sub> ) – α(Cl <sub>7</sub> –C–Cl <sub>8</sub> )	δCCl <sub>3</sub> as´
S <sub>12</sub>	A´´	α(Cl <sub>7</sub> –C–Cl <sub>6</sub> ) – α(Cl <sub>7</sub> –C–Cl <sub>8</sub> )	δCCl <sub>3</sub> as´´
S <sub>13</sub>	A´	α(Cl <sub>6</sub> –C–Cl <sub>8</sub> ) + α(Cl <sub>7</sub> –C–Cl <sub>6</sub> ) + α(Cl <sub>7</sub> –C–Cl <sub>8</sub> ) – α(C–C–Cl <sub>7</sub> ) – α(C–C–Cl <sub>6</sub> ) – α(C–C–Cl <sub>8</sub> )	δCCl <sub>3</sub> s
S <sub>14</sub>	A´´	γ(CCO(=O))	γC=O
S <sub>15</sub>	A´	2α(C–C–Cl <sub>7</sub> ) – α(C–C–Cl <sub>6</sub> ) – α(C–C–Cl <sub>8</sub> )	γCCl <sub>3</sub> ´
S <sub>16</sub>	A´´	α(C–C–Cl <sub>6</sub> ) – α(C–C–Cl <sub>8</sub> )	γCCl <sub>3</sub> ´´
S <sub>17</sub>	A´´	τ(O=C–O–H) + τ(C–C–O–H)	τCOH
S <sub>18</sub>	A´´	τ(O=C–C–Cl <sub>6</sub> ) + τ(O=C–C–Cl <sub>7</sub> ) + τ(O=C–C–Cl <sub>8</sub> ) τ(O–C–C–Cl <sub>6</sub> ) + τ(O–C–C–Cl <sub>7</sub> ) + τ(O–C–C–Cl <sub>8</sub> )	τCCl <sub>3</sub>

<sup>a</sup> See Figure 1 for atom numbering. <sup>b</sup> r, bond distance; α, bond angle; γ, out of the plane angle; τ, torsional dihedral angle; Normalizing constants are not given; they are chosen as  $N = \sum(c_i^2)^{-1/2}$ , where  $c_i$  is the coefficient of the internal coordinate  $i$  contributing to the symmetry coordinate. <sup>c</sup> v, stretching; δ, bending; γ, rocking; τ, torsion.

**Table S3** – B3LYP/cc-PVDZ calculated infrared spectra for *cis*- and *trans*-TCA and results of normal coordinate analysis for both conformers. <sup>a</sup>

<i>cis</i> -TCA				<i>trans</i> -TCA					
Calculated <sup>b</sup> $\nu$	$I^{\text{IR}}$	Approximate Description	Sym- metry	PED/% <sup>c</sup>	Calculated <sup>b</sup> $\nu$	$I^{\text{IR}}$	Approximate Description	Sym- metry	PED/% <sup>c</sup>
3710.4	99.7	$\nu\text{OH}$	A'	S <sub>1</sub> (100)	3720.2	71.1	$\nu\text{OH}$	A'	S <sub>1</sub> (100)
1861.7	246.5	$\nu\text{C=O}$	A'	S <sub>2</sub> (89)	1896.5	220.8	$\nu\text{C=O}$	A'	S <sub>2</sub> (88)
1370.7	48.3	$\delta\text{COH}$ , $\nu\text{C-O}$	A'	S <sub>8</sub> (44) + S <sub>3</sub> (28) + S <sub>9</sub> (16)	1334.2	377.4	$\delta\text{COH}$	A'	S <sub>8</sub> (64) + S <sub>3</sub> (19)
1182.9	191.2	$\nu\text{C-O}$ , $\delta\text{COH}$	A'	S <sub>8</sub> (43) + S <sub>3</sub> (41)	1195.1	11.8	$\nu\text{C-O}$	A'	S <sub>3</sub> (51) + S <sub>8</sub> (29)
940.0	12.9	$\nu\text{CC}$	A'	S <sub>4</sub> (48) + S <sub>3</sub> (17) + S <sub>13</sub> (17) + S <sub>7</sub> (13)	921.9	46.8	$\nu\text{CC}$	A'	S <sub>4</sub> (46) + S <sub>3</sub> (15) + S <sub>13</sub> (15) + S <sub>7</sub> (13)
823.4	38.9	$\gamma\text{C=O}$	A''	S <sub>14</sub> (53) + S <sub>16</sub> (20) + S <sub>6</sub> (15)	835.9	128.5	$\nu\text{CCl}_3$ as'	A'	S <sub>5</sub> (49) + S <sub>10</sub> (15) + S <sub>15</sub> (14)
822.5	186.2	$\nu\text{CCl}_3$ as'	A'	S <sub>5</sub> (53) + S <sub>10</sub> (16) + S <sub>15</sub> (15) + S <sub>11</sub> (11)	813.2	74.3	$\gamma\text{C=O}$	A''	S <sub>14</sub> (52) + S <sub>16</sub> (20) + S <sub>6</sub> (13)
685.5	229.4	$\nu\text{CCl}_3$ as''	A''	S <sub>6</sub> (53) + S <sub>17</sub> (32) + S <sub>14</sub> (11)	678.7	29.3	$\delta\text{OCO}$	A'	S <sub>9</sub> (66) + S <sub>7</sub> (10)
651.3	95.4	$\delta\text{OCO}$	A'	S <sub>9</sub> (61) + S <sub>7</sub> (10)	639.1	133.7	$\nu\text{CCl}_3$ as''	A''	S <sub>6</sub> (68) + S <sub>14</sub> (23)
554.3	22.8	$\tau\text{COH}$	A''	S <sub>17</sub> (64) + S <sub>14</sub> (19) + S <sub>6</sub> (17)	447.8	62.1	$\tau\text{COH}$	A''	S <sub>17</sub> (87) + S <sub>14</sub> (10)
425.7	1.7	$\nu\text{CCl}_3$ s	A'	S <sub>7</sub> (77) + S <sub>4</sub> (14)	422.4	8.9	$\nu\text{CCl}_3$ s	A'	S <sub>7</sub> (39) + S <sub>9</sub> (15) + S <sub>5</sub> (15) + S <sub>10</sub> (12)
413.2	0.6	$\delta\text{CCO}$	A'	S <sub>10</sub> (39) + S <sub>5</sub> (34) + S <sub>9</sub> (10)	416.2	12.4	$\delta\text{CCO}$ , $\nu\text{CCl}_3$ s	A'	S <sub>7</sub> (35) + S <sub>10</sub> (28) + S <sub>5</sub> (22)
288.5	0.1	$\delta\text{CCl}_3$ s	A'	S <sub>13</sub> (70) + S <sub>4</sub> (18)	286.2	0.7	$\delta\text{CCl}_3$ s	A'	S <sub>13</sub> (69) + S <sub>4</sub> (20)
276.2	0.4	$\delta\text{CCl}_3$ as''	A''	S <sub>12</sub> (74) + S <sub>6</sub> (16)	273.6	0.3	$\delta\text{CCl}_3$ as''	A''	S <sub>12</sub> (69) + S <sub>6</sub> (19)
266.4	0.4	$\delta\text{CCl}_3$ as'	A'	S <sub>11</sub> (69) + S <sub>10</sub> (15)	268.9	5.8	$\delta\text{CCl}_3$ as'	A'	S <sub>11</sub> (68) + S <sub>10</sub> (14)
189.0	1.1	$\gamma\text{CCl}_3$ ''	A''	S <sub>15</sub> (65) + S <sub>11</sub> (21) + S <sub>10</sub> (11)	191.7	3.6	$\gamma\text{CCl}_3$ ''	A''	S <sub>15</sub> (57) + S <sub>11</sub> (20)
183.1	0.1	$\gamma\text{CCl}_3$ '	A'	S <sub>16</sub> (69) + S <sub>14</sub> (19) + S <sub>12</sub> (13)	180.1	1.2	$\gamma\text{CCl}_3$ '	A'	S <sub>16</sub> (64) + S <sub>14</sub> (14) + S <sub>12</sub> (12)
37.9	1.4	$\tau\text{CCl}_3$	A''	S <sub>18</sub> (100)	6.3	7.7	$\tau\text{CCl}_3$	A''	S <sub>18</sub> (100)

<sup>a</sup> Wavenumbers ( $\nu$ ) in  $\text{cm}^{-1}$  infrared intensities ( $I^{\text{IR}}$ ) in  $\text{km mol}^{-1}$ . <sup>b</sup> Non-corrected wavenumbers (full spectral range). <sup>c</sup> See Table S2 (Supporting Information) for definition of symmetry coordinates; only PED values equal or larger to 10% are shown.